

Synthesis, Characterization and Gas Sensing Applications of Steel Material using Nanoparticles

Chandrabhas B. Patil^{*},

^{*}Assistant Professor,

Department of Civil Engineering,

Adarsh Institute of Technology and Research Centre,
Vita, Dist. Sangli, Maharashtra, India - 415311.

Shrikant S. Ingale[†]

[†]Assistant Professor,

Department of Civil Engineering,

Adarsh Institute of Technology and Research Centre,
Vita, Dist. Sangli, Maharashtra, India - 415311.

Abstract: Steel constitutes very profitable market for industry. The total turnover of this market is approximately 100 billion US dollars per year. The contribution in this field by the scientists and researchers from USA, Japan, China, Germany and Korea is significant. Very few Indian universities and Institutional laboratories have done some work related to steel synthesis, application and characterizations some of them are mentioned here. The characterization results are matches with International Standard Maps so prepared samples are verified as Steel. The pure steel without doping in any metal is highly sensitive and selective to H₂S gas. The prepared samples show high resistance to corrosion at regular atmospheric condition. We found many applications of sample as selective and sensitive to monitoring Environmental condition and other constructional uses.

Keywords: Sensor, Sensitivity, Gas Sensing, X-ray diffraction, microscopy, spectroscopy.

1. INTRODUCTION:

1.1 General:

Steel is an alloy of iron and carbon that is widely used in construction and other applications because of its hardness and tensile strength. Carbon, other elements, and inclusions within iron act as hardening agents that prevent the movement of dislocations that naturally exist in the iron atom crystal lattices. The carbon in typical steel alloys may contribute up to 2.1% of its weight. Varying the amount of alloying elements, their formation in the steel either as solute elements, or as precipitated phases, retards the movement of those dislocations that make iron so ductile and weak, or thus controls qualities such as the hardness, ductility, and tensile strength of the resulting steel. Steel's strength compared to pure iron is only possible at the expense of ductility, of which iron has an excess. The carbon content of steel is between 0.002% and 2.1% by weight for plain iron-carbon alloys. These values vary depending on alloying elements such as manganese, chromium, nickel, and so on. Basically, steel is an iron-carbon alloy that does not undergo eutectic reaction.

A sensor is a technological device that detects / senses a signal, physical condition and chemical compounds. It is also defined as any device that converts a signal from one form to another. Sensors are mostly electrical or electronic. A sensor acquires a physical parameter and

converts it into a signal suitable for processing (e.g. optical, electrical, mechanical). Sensors are omnipresent.

Gas sensing research initially started with the metal oxide semiconductor which senses a gas when material is heated at higher temperature. Doped or undoped SnO₂ is mostly studied and used among the inorganic materials but its operative temperature is about 423-623K. Since, ZnO and SnO₂ were prepared by co-firing for CO gas sensor. Using property that, sensing gas changes a surface charge carrier concentration of semiconductor to cause change in its conductivity. This helps to monitor hazardous gases and to detect the threshold level of gases present in the atmosphere. However, with respect to the gas response at low concentration of gas, long term stability of these sensors showed poor performance. This increases the power consumption, reduction in sensor life and limits the portability. Therefore, several different approaches have been emerged to overcome these issues. Alternatively, the heterojunction based sensors were constructed due to considerable interest towards several useful applications in switching devices, solar cells, junction field effect transistors and gas sensor. The responses of several different heterojunction sensors to a range of gases including CO or CO₂, H₂, H₂S, NO₂ and C₂H₅OH have been investigated.

1.2 Characteristics of gas sensor:

The gas sensor performance characteristics are divided into sensitivity, repeatability, response time, recovery time and stability; these are most important and deciding parameter for sensor.

i. Sensitivity:

The sensitivity is defined in terms of the relationship between input physical signal and output electrical signal. It is generally, the ratio between a small change in electrical signal to small change in physical signal.

ii. Repeatability:

The ability of a sensor is to reproduce output reading at room temperature, unless otherwise specified when the same measured is applied to it consecutively, under the same conditions and same direction.

iii. Response time and recovery time:

The time taken by sensor to attain 90% of maximum increase in conductance on exposure of the target gas is known as response time. The time taken by the sensor to get back 90% of maximum conductance when the flow of gas is switched off is known as recovery time.

1.3 Gas-Sensing Properties

The working temperature is important for the investigation on gas-sensing properties due to its great influence on the surface state of sensing materials, as well as the contact reactions during the gas-sensing process. The gas sensing study was initiated with a view to study the gas sensing properties of ZnO and AgO thick film resistors with 1, 3, 5, 7 and 10 wt. % Al doping and fired at 700°C. The main characterization is the optimization of operating temperature of film sample for test gases. On the basis of measured data, the sensitivity, selectivity, response and recovery time of thick film sensor for a fixed gas concentration of 1000 ppm in air ambient condition are calculated. Also the response of gas with variation of gas concentration at optimum operating temperature is studied.

1.4 Optimization of operating temperature and Sensitivity of gas sensor

The gas sensing behaviour of ZnO: Al and AgO thick films fired at 700°C was studied by using static measurement system. The DC resistance of ZnO: Al and AgO thick film resistors was measured by using half bridge method as a function of temperature in air as well as in H₂S, LPG, CO₂, NH₃, NO₂, and Ethanol vapour gas atmosphere (1000ppm). The operating temperature was varied at the interval of 50°C. From the measured resistance in air as well as in gas atmosphere, the sensitivity of gas was determined at particular operating temperature using the equation.

2. Methods:

2.1 Method of sample preparation:

Following are the methods used for sample preparation,

- 1) Sol-Gel Method
- 2) Solid State Reaction Method
- 3) Chemical Method (Dip Coating Method)
- 4) Chemical Method (Spin Coating)
- 5) Plasma Reactor Development Method
- 6) E-Beam Evaporation Method

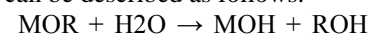
From all above methods, Sol-Gel method is used of sample preparation,

2.1.1 Sol-Gel Method:

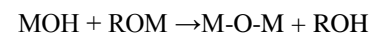
The sol gel process, as the name implies, involves the evolution of inorganic network in a continuous liquid phase (gel). The precursors for synthesizing these colloids consist usually of a metal or metalloid element surrounded by various reactive ligands. The starting material is processed to form a dispersible oxide and forms a sol in contact with water or dilute acid. Removal of the

liquid from the sol yields the gel, and the sol/gel transition controls the particle size and shape. Calcinations of the gel produce the oxide. Sol gel processing refers to the hydrolysis and condensation of alkoxide based precursor.

The reaction involved in the sol gel chemistry based on the hydrolysis and condensation of metal alkoxide M-(OR)_Z can be described as follows:



(hydrolysis)



(condensation)

Sol-gel method of synthesizing nanomaterial is very popular amongst chemists and is widely employed to prepare oxide materials.

The sol-gel process can be characterized by a series of distinct steps:-

Step 1:- Formation of different stable solutions of the alkoxide or the sol.

Step 2:- Gelation is resulting from the formation of the gel by a poly-condensation or poly-esterification reaction that results in a dramatic increase in the viscosity of the solution.

Step 3:- Aging of the gel, during which poly-condensation reaction continues until the gel transforms into a solid mass, accompanied by contraction of the gel network and expulsion of solvent from gel pores.

Step 4:- Drying of the gel, when water and volatile liquids are removed from the gel network. This process is complicated due to fundamental changes in structure of the gel. If isolated by thermal evaporation, the resulting monolith is termed a xerogel. If the solvent is extracted under super critical or near super critical conditions, the product is an aerogel.

Step 5:- Dehydration, during which surface-bound M-OH groups are removed, by their stabilizing the gel against rehydration. This is normally achieved by calcining.

Step 6:- Densification and decomposition of the gels at high temperature. The pores of the gel network collapse and the remaining organic species are volatilized.

2.2 Methods of Characterization:

Characterization of nanoparticles in national level research institute. These tests are listed out below:

- a) X-ray diffraction (XRD),
- b) Scanning electron microscopy (SEM),
- c) Transmission electron microscopy (TEM),
- d) Energy dispersive spectroscopy (EDS),
- e) UV-visible spectroscopy (UV-Vis),
- f) Hardness tester.

2.2.1 X-ray diffraction (XRD):

X-rays are the electromagnetic radiations with wavelength in the range between 0.01-1.0 nm. They travel in a straight line with the velocity of light, $c = 299792458$ m/s, and they have enough energy to travel through sufficiently thin solids. Their discovery is attributed to the German Physicist Rontgen in 1896. In the electromagnetic spectrum X-rays are located in between ultraviolet rays and Gamma rays. It is known from Quantum mechanics that

electromagnetic radiation can be regarded as either a wave or a particle. Generation and Properties of X-rays Theory of electromagnetism predict that electromagnetic radiations will be produced whenever a charged particle is accelerated or decelerated. When a beam of high energy electrons is created and then abruptly brought to halt, and then those electrons will emit part or all of their energy in the form of X-rays. This is called braking-radiation or Bremsstrahlung. When a high potential is maintained between two electrodes; electrons are introduced into the field, and by virtue of their negative charge, electrons are attracted to the positive electrode. An electron starting from negative electrode will have energy when it reaches the positive electrode; here it suffers an abrupt stoppage, creating X-rays.

2.2.2 Scanning Electron Microscope (SEM):

The scanning electron microscope (SEM) is a type of electron microscope that images the sample surface by scanning it with a high-energy beam of electrons in a raster scan pattern. The electrons interact with the atoms that make up the sample producing signals that contain information about the sample's surface topography, composition and other properties such as electrical conductivity. The types of signals produced by an SEM include secondary electrons, back-scattered electrons (BSE), characteristic X-rays, light (cathodoluminescence), specimen current and transmitted electrons.

Secondary electron detectors are common in all SEMs, but it is rare that a single machine would have detectors for all possible signals. The signals result from interactions of the electron beam with atoms at or near the surface of the sample. In the most common or standard detection mode, secondary electron imaging or SEI, the SEM can produce very high-resolution images of a sample surface, revealing

details about less than 1 to 5 nm in size. Due to the very narrow electron beam, SEM micrographs have a large depth of field yielding a characteristic three-dimensional appearance useful for understanding the surface structure of a sample.

2.2.3 Transmission electron microscopy (TEM):

Transmission electron microscopy is a technique whereby a beam of electrons is transmitted through an ultra-thin specimen, interacting with the specimen as it passes through. An image is formed from the interaction of the electrons transmitted through the specimen; the image is magnified and focused onto an imaging device, such as a fluorescent screen, on a layer of photographic film, or to be detected by a sensor such as a CCD camera. TEMs are capable of imaging at a significantly higher resolution than optical microscopes, owing to the small de Broglie wavelength of electrons. This enables the instrument's user to examine fine detail-even as small as a single column of atoms, which is tens of thousands times smaller than the smallest resolvable object in a light microscope. TEM forms a major analysis method in a range of scientific fields, in both physical and biological sciences. TEMs find application in cancer research, virology, materials science as well as pollution and semiconductor research. At smaller magnifications TEM image contrast is due to absorption of electrons in the material, due to the thickness and composition of the material. At higher magnifications complex wave interactions modulate the intensity of the image, requiring expert analysis of observed images. Alternate modes of use allow for the TEM to observe modulations in chemical identity, crystal orientation, electronic structure and sample induced electron phase shift as well as the regular absorption based imaging.

2.3 Steps involved during preparation of sample:



Figure 1: Preparation of sample (Zn & Ag)

2.3.1 Sample No. 1:

Preparation of nanoparticles of steel nanoparticle—→Making a homogeneous mixture of [Ferrous nitrate AR + Di-Ammonium hydrogen ortho-phosphate + Chromium Nitrate AR] —→Heating a mixture at 70-90⁰C temperature—→In magnetic stirrer with heater about 25-30min—→Combustion will carried out Escaping of impurities and gasesLike N₂, O₂, CO₂ etc.—→Cooling at room temperature about 10 min —→Solid form power heated at 1100⁰C temperature—→Muffle furnace about 6 hours —→Nanoparticles of steel nanoparticle composite material in power Form is obtained.

2.3.2 Sample No.2:

Preparation of nanoparticles of Zn doped steel nanoparticle —→Making a homogeneous mixture of [Ferrous nitrate AR + Di-Ammonium hydrogen ortho-phosphate +Chromium Nitrate AR + Zinc Nitrate] —→Heating a mixture at 70-90⁰C temperature —→ In magnetic stirrer with heater about 25-30min —→ Combustion will carried out Escaping of impurities and gases like N₂, O₂, and CO₂ etc. —→ Cooling at room temperature about 10 min —→ Solid form power heated at 1100⁰C temperature in —→

Muffle furnace about 6 hours —→ Nanoparticles of steel nanoparticle composite material in power Form is obtained

2.3.3 Sample No. 3:

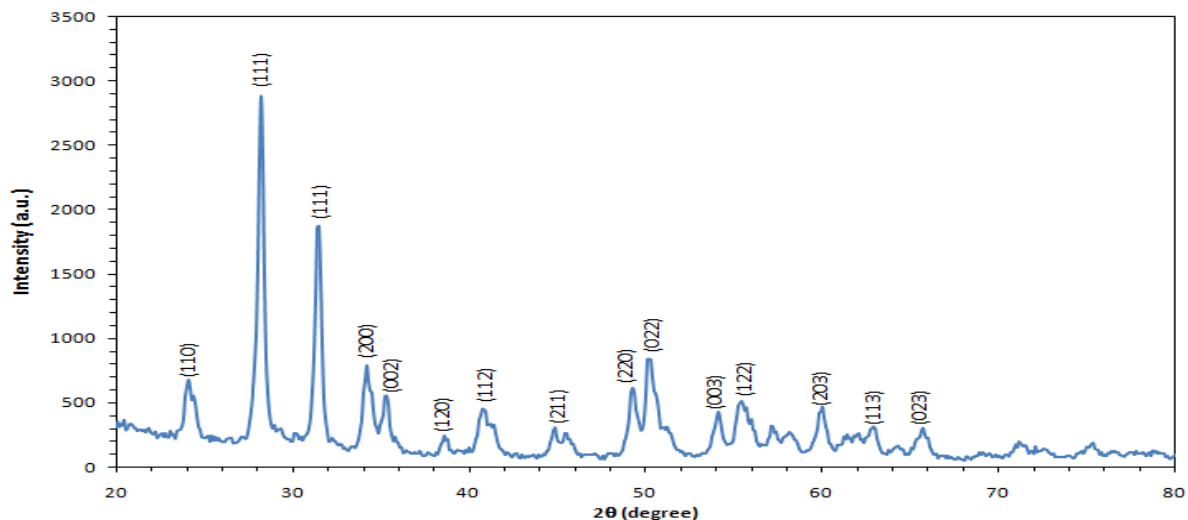
Preparation of nanoparticles of Ag doped steel nanoparticle —→ Making a homogeneous mixture of [Ferrous nitrate AR + Di-Ammonium hydrogen ortho-phosphate +Chromium Nitrate AR+ Silver Nitrate] —→ Heating a mixture at 70-90⁰C temperature —→ In magnetic stirrer with heater about 25-30min —→ Combustion will carried out Escaping of impurities and gases like N₂, O₂and CO₂ etc. —→ Cooling at room temperature about 10 min —→ Solid form power heated at 1100⁰C temperature in —→ Muffle furnace about 6 hours. —→ Nanoparticles of steel nanoparticle composite material in power Form is obtained.

3. RESULTS AND DISCUSSION:

3.1 Sample No. 1:

3.1.1 X-ray diffraction (XRD):

Graph 1shows the X-ray Diffractogram (XRD) of the porous steelnano powder. The observed peaks match well with the standard JCPDS data of porous steel. The broad peaks are due to the nano-crystalline nature of porous steel.



Graph No.1: X-ray Diffractogram (XRD)

Scherrers Formula for Grain Size is, $t = 0.9\lambda / \beta \cos\theta$
Where, λ =wavelength of X-ray;
 β = FWHM of peak;
 θ =corresponding angle of peak.

The average grain size calculated from Scherrers formula was about 18 nm.

3.1.2 Surface Topography Using SEM:

Scanning electronmicrograph is shown in figure 1 by using topography of the film surface. Scanning electron microscope could not resolve nanoparticles associated with the film even at very high magnification. It may be due to

very small nano-crystalline particles associated with the film.The quantitative elemental composition of the steel was analyzed using an energy dispersive spectrometer (EDS).Observed at% of Fe and O is: 30.33 and 69.67, respectively. There is little deviation from stoichiometry of the prepared film.

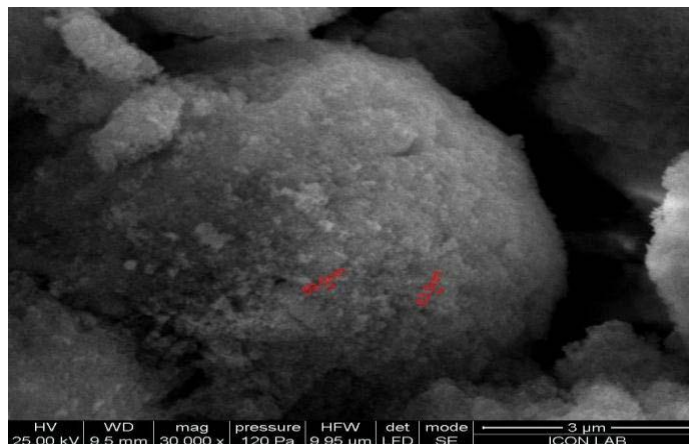


Figure 2: Scanning electron micrograph of nano-crystalline steel.

3.1.3 Transmission Electron Microscopy (TEM):

The TEM technique was used to know the exact grain size, shape, and distribution of the crystallites

associated with the powder. It is clear from the TEM image Fig.2 that there are uniformly distributed grains with an average grain size of 20 nm.

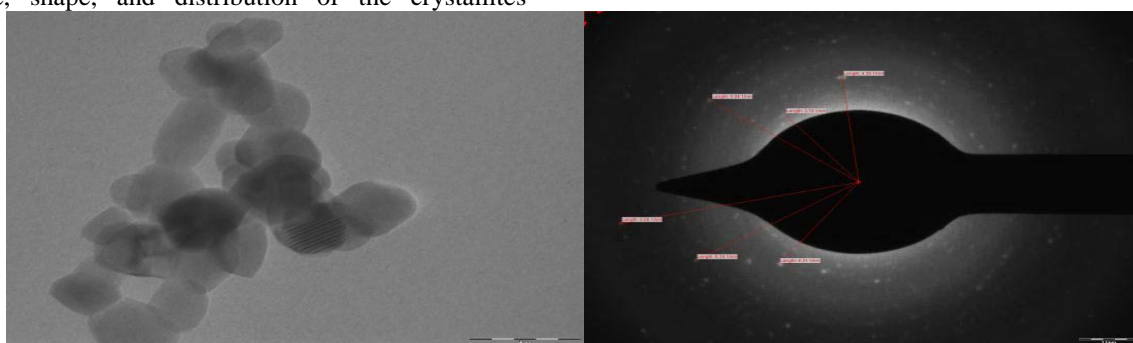
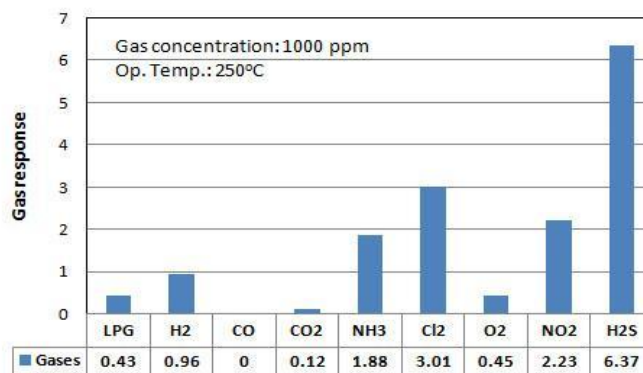


Figure 3: Transmission electron micrograph Figure 4: SAED pattern of nano-crystalline steel.

Additional structural characterization of porous steel nanopowder was carried out by electron diffraction shown in Fig. 3 Spherical rings in electron diffraction

patterns suggest that the nanopowder has good crystallinity. The images clearly show the spotty fringes corresponding to the lattice planes of porous steel.

3.1.4 Selectivity of Sensor:



Graph No 2: Selectivity of porous steel sensor

Selectivity can be defined as the ability of a sensor to respond to a certain gas in the presence of different gases. It is observed from graph 5.4 that the porous steel thick film sensor gives maximum response to H₂S (1000 ppm) at 250°C. The sensor showed highest selectivity for H₂S against all other tested gases: NH₃, LPG, Cl₂, CO, CO₂, O₂, H₂ and NO₂. Hence it is highly selective to H₂S gas.

- **Response Time and Recovery Time:**
The response/ recovery time is an important parameter used for characterizing a sensor. It is defined as the time required to reach 90% of the final change in current, when the gas is turned on and off respectively. The response was quick (8 sec) while the recovery was fast (<

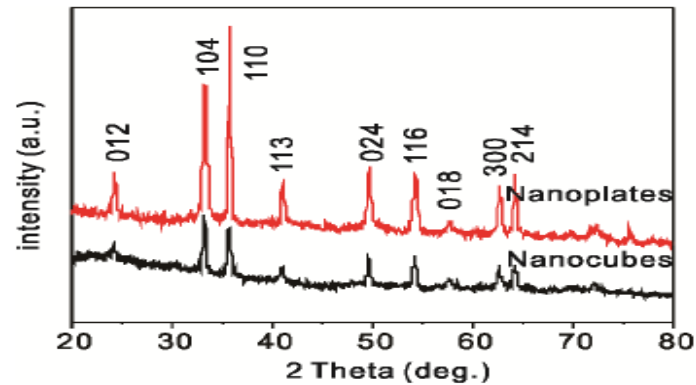
18 sec). The quick response may be due to faster oxidation of gas.

3.2 Sample No. 2

3.2.1 X-ray diffraction (XRD):

The phase of the as-prepared asteel nanoparticles and Zn-steel nanoparticles were characterized using X-ray

diffraction. All the diffraction peaks of the products in the graph 5.5 were in agreement with the standard data of steel nanoparticles (JCPDS No. 33-0664).



Graph No. 3: XRD patterns of the as-prepared Zn-steel nanoparticles nanostructures

3.2.2 SEM & TEM:

The morphology and crystallinity of the as-prepared Zn-steel nanoparticles were analyzed using scanning electron microscopy (SEM), transmission electron microscopy (TEM), and high-resolution TEM (HRTEM). SEM and TEM images for nanocubes and hexagonal nanoplates are shown in Fig. 5.4

All of the nanoplates display a well-defined hexagonal shape. Based on a SEM and TEM analysis, the width of the plates is determined to be about 130 nm. A representative HRTEM image (Fig. c) and the SAED

pattern (inset in Fig. c) show the lattice fringe to be 0.25 nm, which is consistent with (110), (120), and (210) planes, respectively. The resulting basal plane is (001). A TEM image (Fig. e) shows that α -Fe₂O₃ nanocubes appear to be square in shape with an average size of about 25 nm. A HRTEM image (Fig. f) and corresponding SAED (inset in Fig. f) indicate that the lattice fringe is 0.36 nm and the dihedral angle is 86°, corresponding to (012) plane. Thus, the dominant exposed facets of the nanoplates and nanocubes are {001} and {012}, respectively.

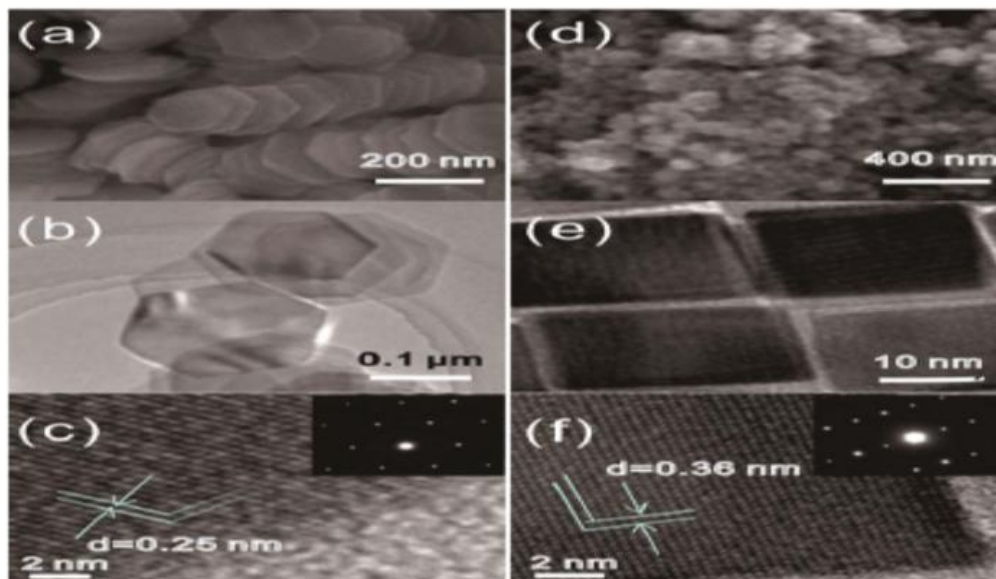
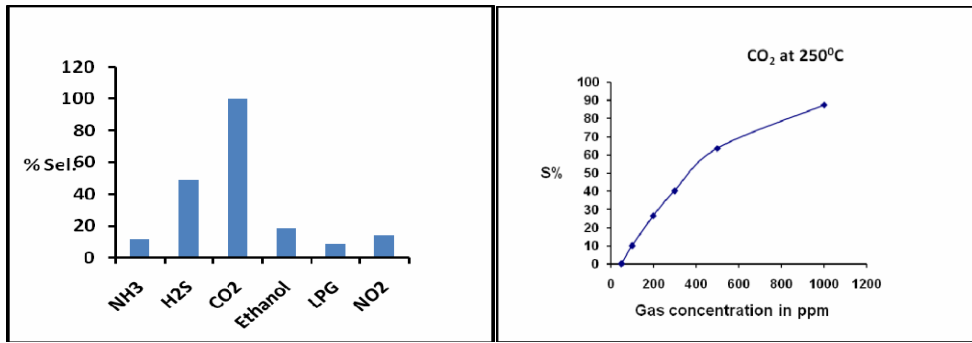


Figure No. 5: Representative Morphologies and structures of Zn-steel nanoparticles.

- (a) SEM image, (b) TEM image, (c) HRTEM image of Zn-steel nanoparticles. Insets: SAED pattern. (d) SEM image, (e) TEM image and (f) HRTEM image Zn-steel nanoparticles. Insets: SAED pattern.

3.2.3 Selectivity of 10 Wt. % Al Doped ZnO Thick Films:



Graph No. 4: ZnO thick film is highly selective to CO₂ gas and less selective to the LPG.

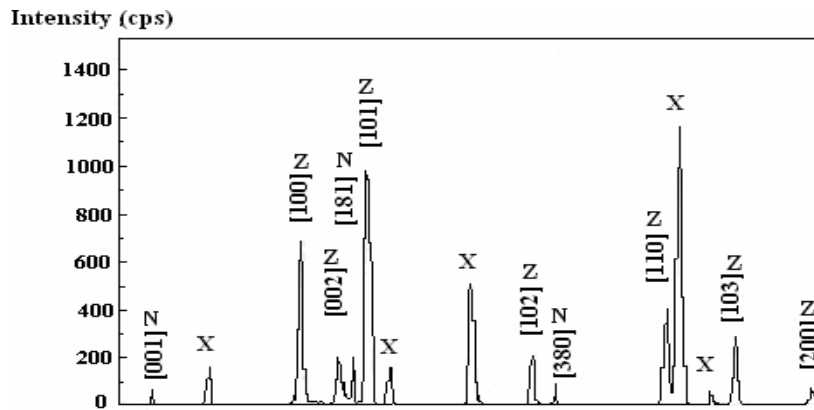
Graph No. 5: shows variation of sensitivity of 10 wt. % AL doped ZnO thick films with CO₂ concentration in ppm level at the optimum temperature 250°C.

The 10 wt. % Al doped ZnO films were exposed to different concentrations of CO₂. The sensitivity values were observed to have increased by increasing the gas concentration up to 1000 ppm. The response was highest for 1000 ppm of CO₂. From the above graph 5.13, it has

been observed that the sensitivity of thick films for CO₂ at 250°C increases linearly with increase in gas concentration upto 500 ppm. Above 500 ppm the increase in sensitivity is slow and almost saturates at 1000 ppm.

3.3 Sample No. 3:

3.3.1 X-ray diffraction (XRD):



Graph No. 6: XRD pattern of AgO thick films

3.3.2 SEM:

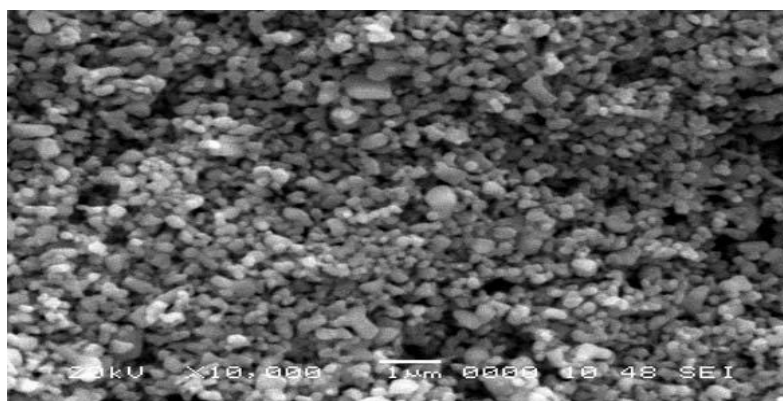
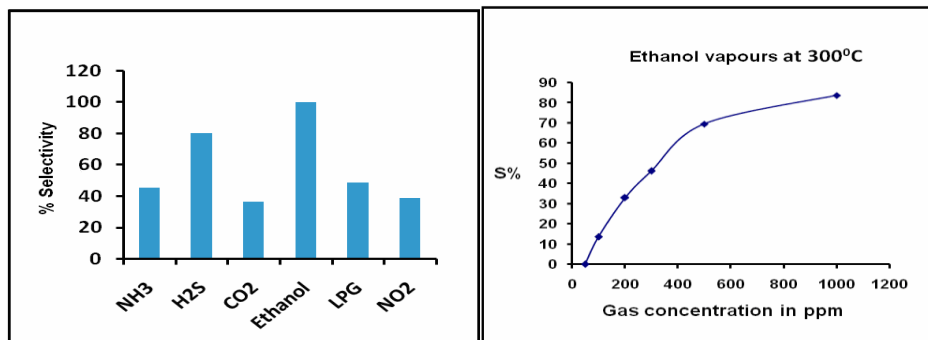


Figure No.6: Scanning Electron Microscopy

The microstructure observation revealed that the AgO addition retarded the grain growth. The grain size of pure steel films is more than AgO doped steel films.

3.3.3 Selectivity AgO thick films for different gases:



Graph no.7: Shows the selectivity of AgO thick films for

Graph no.8: Shows the selectivity of AgO thick films for different

different gases against Ethanol vapour at 300°C against Ethanol vapour at 300°C

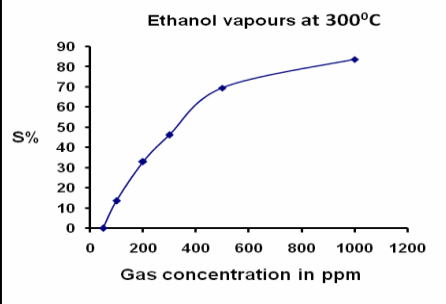
The films were exposed to different concentrations of Ethanol vapour. The sensitivity values were observed to have increased by increasing the gas concentration up to 1000 ppm. The response was highest for 1000 ppm of Ethanol vapour. From the above graph 5.20, it has been observed that the sensitivity of 3 wt. AgO doped steel thick films for Ethanol vapour at 300°C increases linearly with increase in gas concentration upto 500 ppm. Above 500 ppm the increase in sensitivity is slow and almost saturates at 1000 ppm. Thus the active region of the sensor would be up to 500 ppm. At lower gas concentrations, the monomolecular layer of gas molecules would be formed on the surface of the sensor which could interact more actively giving larger response. At the higher gas concentrations, the multilayer of gas molecules may be formed that would result into saturation in response beyond 500 ppm.

3.4 Applications of Gas Sensors:

- i. Industrial production (e.g. methane detection in soil mines)
- ii. Environmental studies (e.g., greenhouse gas monitoring)
- iii. Indoor air quality supervision (e.g., detection of carbon monoxide)
- iv. Automotive industry (e.g. detection of polluting gases from vehicles)
- v. In construction
- vi. Medical applications (e.g. electronic noses simulating the human olfactory system)
- vii. Process control industries
- viii. Boiler control
- ix. Fire detection
- x. House safety

4. CONCLUSIONS:

1. In this way we prepare samples of Steel with inclusion of CNT using Sol-gel Autocombustion method.
2. The characterization results are matches with International Standard Maps so prepared samples are verified as Steel.
3. The pure steel without doping in any metal is highly sensitive and selective to H₂S gas
4. The sample doped in zinc is highly sensitive and selective to CO₂ gas.



5. The sample doped in silver is highly sensitive and selective to Ethanol gas.
6. The prepared samples show high resistance to corrosion at regular atmospheric condition.
7. We found many applications of sample as selective and sensitive to monitoring Environmental condition and other constructional uses.

5. REFERENCES:

Journals:

1. C.H. Wang, X.F. Chu, and M.W. Wu (2013), "Detection of H₂S down to ppm levels at room temperature using sensors based on steel Nanorods, sensors and actuators B-chemical", page no. 113-120.
2. A. M. K. Esawi, K. Morsi, A. Syed, A. Abdel Gawad, P. Borah (2009), "Fabrication and properties of dispersed carbon nanotubes-aluminium composites", Material Science and Engineering, page no. 167-173.
3. C. F. Hsu, H. M. Lin and P.Y. Lee (2008), "Advance Engineering materials", page no. 1053-1055.
4. A.K. Srivastava, C. L. Xu, B. Q. Wei, R. Kishore and K. N. Sood (2008), "Microstructural features and mechanical properties of carbon nanotubes reinforced aluminium-based metal matrix composite", Indian journal of Engineering and Material Science, Volume 15, page no. 247-255.
5. M.S. Wagh, G.H. Jain, D.R. Patil, S.A. Patil, L.A. Patil (2006), "Sensors and actuators B-115", page no. 128-139.
6. C. L. Xu, B. Q. Wei, R. Z. Ma, J. Liang, X. K. Ma and D. H. Wu (1999), "Fabrication of aluminium-carbon nanotubes composites and their electrical properties", volume 37, page no. 855-858.
7. Y. Zhao, X.L. He, J.P. Li, X.G. Gao, J. Jia, "Steel doped CuO/SnO₂ composite nanofibers fabricated by electrospinning and their H₂S sensing properties," Sensor Actuat B-Chem, vol. 165, pp. 82-87, 2012.
8. C.R. Michel, N.L.L. Contreras, A.H. Martinez-Preciado, "Gas sensing properties of nanostructured bismuth oxychloride," Sensor Actuat B-Chem, vol. 160, pp. 271-277, 2011.
9. S.Q. Tian, F. Yang, D.W. Zeng, C.S. Xie, "Solution-Processed Gas Sensors Based on ZnO Nanorods Array with an Exposed (0001) Facet for Enhanced Gas-Sensing Properties," J PhysChem C, vol. 116, pp. 10586-10591, 2012.